

Perceptually Optimized Coding of Color Images for Band-Limited Information Networks

Evgeny Gershikov

Department of Electrical Engineering, Ort Braude Academic College of Engineering, Karmiel, Israel
and Department of Electrical Engineering, Technion – IIT, Haifa, Israel
eugeny@tx.technion.ac.il

Abstract

The Mean Square Error (MSE) or the Peak Signal to Noise Ratio (PSNR) are common distortion measures used to assess image quality. Nevertheless, they are usually chosen due to their simplicity and not their performance as they are not always suitable compared to the human observer. In this work we present a Rate-Distortion approach to color image compression based on subband transforms using perceptual optimization of the compression quality. This approach is based on minimization of the Weighted Mean Square Error (WMSE) of the encoded image, which better corresponds to the quality assessment of the human eye. The WMSE can be measured in the YCbCr color space, for which visual weights are relatively easily derived. Based on the new approach, new optimized compression algorithms are introduced using the Discrete Cosine Transform and the Discrete Wavelet Transform. We compare the new algorithms to presently available algorithms such as JPEG and JPEG2000. Our conclusion is that the new WMSE optimization approach outperforms presently available compression systems when a human observer is considered.

Keywords

Color Image Compression; Weighted Mean Square Error; Discrete Cosine Transform; Discrete Wavelet Transform; Perceptual Rate-Distortion Model; Optimal Color Component Transform; Optimal Rate Allocation

Introduction

Many color image coding algorithms are based on subband transforms for the compression process. The complexity of such algorithms varies from systems based on elementary block transforms like the DCT (Discrete Cosine Transform) [14] used, for example, in JPEG [21] to more complicated algorithms based on the Lapped Biorthogonal Transform (LBT), the Discrete Wavelet Transform (DWT), wavelet packets and filter banks, such as EZW (Embedded Zerotree Wavelet)[19], JPEG2000 [13][15], JPEG XR [2][16] or

uniform DFT filter banks [18]. Still it is not always clear that the added complexity also improves the compression results. The recently introduced Rate-Distortion (R-D) model for subband transform coders [5] can be used in such applications to assess the performance of the compression algorithm. This R-D model, however, approximates the MSE distortion of the compression results, which is not always well correlated with subjective image quality as seen by the human eye. More complicated distortion measures can be proposed, such as calculating the MSE distortion between two images after an intensity transformation and filtering for gray-scale images [11] or a similar process using a non-linear transformation of the primary color components, followed by filtering, for a color image [1]. A basic measure that is similar to the MSE, but can incorporate perceptual weights is the Weighted MSE (WMSE). This measure assigns a different weight to the MSE of each subband of the image, thus simulating the varying sensitivity of the Human Visual System (HVS) to different horizontal and vertical spatial frequencies. As a more realistic tool, it can improve the assessment of the model.

The goal of this work is to develop a perceptual Rate-Distortion (R-D) model of subband transform coders based on the WMSE as the distortion measure. We demonstrate the efficiency of the new model for subband transform coding by presenting a new type of compression algorithms based on perceptual optimization of the pre-processing stage and of the subband rates allocation.

Objective Rate-Distortion Theory of Subband Transform Coders

Consider a general subband transform coder for color images. Typically, the image samples are first pre-processed, then subband transformed and quantized and finally post-processed losslessly. A detailed description of these stages is given below.

1) Pre-processing

Here a CCT (Color Components Transform) is applied to the RGB color components of the image. We denote the RGB components in vector form as $\mathbf{x} = [R \ G \ B]^T$ and the new color components as $\tilde{\mathbf{x}} = [C_1 \ C_2 \ C_3]^T$. The 3×3 size CCT matrix is denoted as \mathbf{M} . This stage can be written as:

$$\tilde{\mathbf{x}} = \mathbf{M}\mathbf{x}. \quad (1)$$

The goal of using the CCT transform is usually to decorrelate the highly correlated RGB components [7][10][15][23]. The CCT transform is often followed by level shifting as for example is the case in JPEG2000 [13] so that the sample range of values becomes symmetric around zero.

2) Subband Transforming and Quantizing

A subband transform, such as the DCT or the DWT is applied to each color component. The subband coefficients of each color component are then quantized. An independent uniform scalar quantizer for each subband is used.

3) Post-processing

The quantized coefficients are encoded losslessly. The goal is to reduce the number of bits required for the coefficients without loss of information. Techniques such as run-length encoding, zero trees, delta modulation and entropy coding are used here. This stage has to be adapted to the subband transform used.

To derive the R-D behavior of the algorithm, first the R-D of a scalar uniform quantizer needs to be considered. Assuming that a random signal x with variance σ_x^2 is quantized by such a quantizer, its Rate-Distortion behavior has been approximated by [6][20]:

$$d(R) = \varepsilon^2 \sigma_x^2 2^{-2R}, \quad (2)$$

where R is the rate and ε^2 is a constant dependent upon the distribution of x . Then based on (2) the R-D model of a general monochromatic subband coder with B subbands can be expressed as:

$$d^{SC}(\{R_b\}) = \sum_{b=0}^{B-1} \eta_b G_b d_b(R_b) = \sum_{b=0}^{B-1} \eta_b G_b \sigma_b^2 \varepsilon^2 e^{-2R_b}. \quad (3)$$

Here d_b is the MSE of subband ($b \in 0, 1, \dots, B-1$), σ_b^2 is its variance, G_b is its energy gain [20] and R_b is the rate allocated to it. Also η_b is its sample rate, i.e., the relative part of the number of coefficients in it from the total number of samples in the signal. α is a constant equal to $2 \ln 2$.

Consider now a color image. The coding algorithm described in the beginning of this section may be regarded as applying a CCT to the image, followed by monochromatically subband coding each of the new color components. The Rate-Distortion model of this algorithm is [2]:

$$d(\{R_{bt}\}, \mathbf{M}) = \frac{1}{3} \sum_{i=1}^3 \sum_{b=0}^{B-1} \eta_b G_b \sigma_{bt}^2 \varepsilon_i^2 e^{-2R_{bt}} ((\mathbf{M}\mathbf{M}^T)^{-1})_{ii}, \quad (4)$$

where σ_{bt}^2 and R_{bt} have the same meaning as before, but for subband b of color component i ($i \in 1, 2, 3$). Optimal rates allocation for the subbands can be found by minimizing the expression of Equation (4) under the rate constraint:

$$\sum_{i=1}^3 \alpha_i \sum_{b=0}^{B-1} \eta_b R_{bt} = R \quad (5)$$

for some total image rate R . Here down-sampling factors α_i have been used. α_i denotes how much the number of samples of color component i has been reduced by down-sampling. For example, if the down-sampling is by a factor of 2 horizontally and vertically then:

$$\alpha_i = \begin{cases} 1 & \text{full component} \\ 0.25 & \text{down-sampled component} \end{cases}$$

The optimal rates under the rate constraint of (5) as well as non-negativity constraints are:

$$R_{bi} = \frac{R}{\sum_{j=1}^3 \alpha_j \xi_j} + \frac{1}{\alpha} \ln \left(\frac{\frac{\varepsilon_i^2 G_b \sigma_{bt}^2 ((\mathbf{M}\mathbf{M}^T)^{-1})_{ii}}{\alpha_i}}{\prod_{k=1}^3 \left(\frac{((\mathbf{M}\mathbf{M}^T)^{-1})_{kk} \varepsilon_k^2 G M_k^{Act}}{\alpha_k} \right)^{\frac{\alpha_k \xi_k}{\sum_{j=1}^3 \alpha_j \xi_j}}} \right), \quad (6)$$

$$R_{bt} = \frac{R}{\sum_{j=1}^3 \alpha_j \xi_j} + \frac{1}{\alpha} \ln \left(\frac{\frac{\varepsilon_i^2 G_b \sigma_{bt}^2 ((\mathbf{M}\mathbf{M}^T)^{-1})_{ii}}{\alpha_i}}{\prod_{k=1}^3 \left(\frac{((\mathbf{M}\mathbf{M}^T)^{-1})_{kk} \varepsilon_k^2 G M_k^{Act}}{\alpha_k} \right)^{\frac{\alpha_k \xi_k}{\sum_{j=1}^3 \alpha_j \xi_j}}} \right) \quad (b \in$$

$$Act_i) \quad R_{bt} = \frac{R}{\sum_{j=1}^3 \alpha_j \xi_j} + \frac{1}{\alpha} \ln \left(\frac{\frac{\varepsilon_i^2 G_b \sigma_{bt}^2 ((\mathbf{M}\mathbf{M}^T)^{-1})_{ii}}{\alpha_i}}{\prod_{k=1}^3 \left(\frac{((\mathbf{M}\mathbf{M}^T)^{-1})_{kk} \varepsilon_k^2 G M_k^{Act}}{\alpha_k} \right)^{\frac{\alpha_k \xi_k}{\sum_{j=1}^3 \alpha_j \xi_j}}} \right)$$

$(b \in Act_i)$, Where $b \in Act_i$ with Act_i denoting the set of non zero (or active) rates in the color component i , i.e.,

$$Act_i \triangleq \{b \in [0, B-1] | R_{bi} > 0\}. \quad (7)$$

Also

$$\xi_i \triangleq \sum_{b \in Act_i} \eta_b, \quad GM_i^{Act} \triangleq \prod_{b \in Act_i} (G_b \sigma_{bi}^2)^{\frac{\eta_b}{\xi_i}}. \quad (8)$$

The structure of this work is as follows. In the next section the perceptual Rate-Distortion model is introduced. Section "Perceptually Optimized Compression" presents new color compression algorithms optimized according to this model based on the DCT subband transform and on the DWT. Simulations of the new algorithms and comparison to presently available algorithms are provided in this section. Our conclusions and summary are given in the final section.

The Perceptual R-D Model

We assume here that we are given the visual perception weights corresponding to the subbands of a certain subband transform (SBT) in a color space. Such a space can be, for example, YCbCr as we have chosen in this work. We now wish to derive an expression for the WMSE distortion of a coder based on the subband transform. The same coder described in Subsection "Objective Rate-Distortion theory of subband transform coders" is assumed, so that a CCT is applied to the RGB color components of the image prior to coding and the actual image data compression is performed in another color space denoted C1C2C3. We denote as $Y_b = [y_b^Y \ y_b^{Cb} \ y_b^{Cr}]^T$ the vector of the SBT coefficients at some index in subband b in the YCbCr color space. Similarly, the vector of subband b coefficients in the C1C2C3 color space is denoted $\tilde{Y}_b = [\tilde{y}_b^{C_1} \ \tilde{y}_b^{C_2} \ \tilde{y}_b^{C_3}]^T$. Due to the linearity of the SBT, the following relationship holds:

$$\tilde{Y}_b = \tilde{M} Y_b \Rightarrow Y_b = \tilde{M}^{-1} \tilde{Y}_b, \quad (9)$$

where \tilde{M} stands for the CCT matrix from the YCbCr color space to the C1C2C3 space. If M is the CCT matrix from RGB to C1C2C3 and M_{YCbCr} is the RGB to YCbCr matrix, then:

$$\tilde{M} = M \cdot M_{YCbCr}^{-1}. \quad (10)$$

Since the SBT coefficients are lossy encoded, errors are introduced between the reconstructed coefficients Y_b^{rec} in the YCbCr color space and the original ones. The error covariance matrix for the subband b in the YCbCr domain is:

$$E\eta_b = E[(Y_b - Y_b^{rec})(Y_b - Y_b^{rec})^T], \quad (11)$$

where $E()$ denotes statistic mean. Similarly in the C1C2C3 domain:

$$\tilde{E}\tilde{\eta}_b = E[(\tilde{Y}_b - \tilde{Y}_b^{rec})(\tilde{Y}_b - \tilde{Y}_b^{rec})^T], \quad (12)$$

and using (9) we can express $\tilde{E}\tilde{\eta}_b$ by $E\eta_b$ as:

$$E\eta_b = \tilde{M}^{-1} \tilde{E}\tilde{\eta}_b \tilde{M}^{-T}. \quad (13)$$

The MSE distortions d_{bi} of the YCbCr color components in subband b are the diagonal elements of $E\eta_b$ and thus:

$$d_{bi} = n_i^T \tilde{E}\tilde{\eta}_b n_i, \quad (14)$$

where n_i is the i^{th} row of \tilde{M}^{-1} in column form. In a similar fashion, the diagonal elements of $\tilde{E}\tilde{\eta}_b$ can be recognized as the MSE distortions \tilde{d}_{bk} of the C_1, C_2, C_3 color components, given by (2) and slightly rewritten to become:

$$\tilde{d}_{bk} = \varepsilon_k^2 \sigma_{bk}^2 e^{-\alpha R_{bk}}, \quad (15)$$

where $\alpha = 2 \ln 2$ and R_{bi} and σ_{bi}^2 , $i \in \{1, 2, 3\}$ denote the rate and variance of subband b of color component C_i respectively. Note that we continue here with the consistent notation of a tilde for the variables related to the C1C2C3 color space. Assuming that the quantization errors of the three color components in each subband in the C1C2C3 domain are uncorrelated, $\tilde{E}\tilde{\eta}_b$ becomes a diagonal matrix and (14) becomes

$$d_{bi} = \sum_{k=1}^3 n_{ik}^2 \tilde{d}_{bk} = \sum_{k=1}^3 (\tilde{M}^{-1})_{ik}^2 \varepsilon_k^2 \sigma_{bk}^2 e^{-\alpha R_{bk}} \quad (16)$$

once (15) is substituted for \tilde{d}_{bk} . Now if, for the sake of convenience, we denote the YCbCr components at each pixel as a vector $x^{YCbCr} = [Y \ Cb \ Cr]^T$, then the WMSE of the i^{th} color component $(x^{YCbCr})_i$ is:

$$WMSE((x^{YCbCr})_i) = \sum_{b=0}^{B-1} \eta_b G_b w_{bi} d_{bi} \quad (17)$$

As can be seen, this expression incorporates the energy gains of the subbands G_b as well as their sample rates η_b . Also the visual weights w_{bi} are part of the expression, providing varying significance to different subbands of the same color component as well as between color components. Defining the total WMSE as the average WMSE of the YCbCr color components, we get:

$$\begin{aligned} WMSE &= \frac{1}{3} \sum_{i=1}^3 WMSE((x^{YCbCr})_i) \\ &= \frac{1}{3} \sum_{i=1}^3 \sum_{b=0}^{B-1} \eta_b G_b w_{bi} d_{bi} \end{aligned} \quad (18)$$

and after substituting (16) for d_{bi} the expression becomes:

$$WMSE = \frac{1}{3} \sum_{i=1}^3 \sum_{b=0}^{B-1} \eta_b G_b w_{bi} \sum_{k=1}^3 \left(\bar{\mathbf{M}}^{-1} \right)_{ik}^2 \varepsilon_k^2 \sigma_{bk}^2 e^{-aR_{bk}} \quad (19)$$

$$= \frac{1}{3} \sum_{b=0}^{B-1} \eta_b G_b \sum_{k=1}^3 \varepsilon_k^2 \sigma_{bk}^2 e^{-aR_{bk}} \sum_{i=1}^3 w_{bi} \left(\bar{\mathbf{M}}^{-1} \right)_{ik}^2.$$

To simplify (19) we denote:

$$\psi_{bk} \triangleq \sum_{i=1}^3 w_{bi} (\bar{\mathbf{M}}^{-1})_{ik}^2 \quad (20)$$

so that the WMSE expression becomes:

$$WMSE = \frac{1}{3} \sum_{b=0}^{B-1} \sum_{k=1}^3 \eta_b G_b \sigma_{bk}^2 \varepsilon_k^2 e^{-aR_{bk}} \psi_{bk}. \quad (21)$$

Clearly, if the visual weights w_{bi} are all equal to 1, the WMSE expression of (21) should become the expression for the MSE in the YCbCr domain. This expression is given exactly by (4) with the difference that \mathbf{M} there is to be replaced by $\bar{\mathbf{M}}$ in our case. From the comparison of equations (21) and (4) we conclude that $\psi_{bk} = ((\bar{\mathbf{M}}\bar{\mathbf{M}}^T)^{-1})_{kk}$ in that case, which means according to (20) that

$$\sum_{i=1}^3 (\bar{\mathbf{M}}^{-1})_{ik}^2 = ((\bar{\mathbf{M}}\bar{\mathbf{M}}^T)^{-1})_{kk}. \quad (22)$$

A straightforward check proves that this is indeed the case.

De-correlation of the Quantization Errors

In the derivation of the WMSE expression of (21) we have assumed that the quantization errors of the \mathbf{C}_1 , \mathbf{C}_2 , \mathbf{C}_3 color components are uncorrelated in each subband. It is of interest to note that the assumption in the derivation of the MSE expression of (4) was the lack of correlation of the quantization errors in the image domain [2], i.e. that $\mathbf{C}_i - \mathbf{C}_i^{rec}$ and $\mathbf{C}_j - \mathbf{C}_j^{rec}$ have zero correlation for $i, j \in \{1, 2, 3\}$, $i \neq j$. Note that \mathbf{C}_i^{rec} denotes here the reconstructed \mathbf{C}_i component. The question that rises is whether the assumption of zero correlation in each subband means also zero correlation in the image domain.

Using the vector space interpretation of subband transforms [20], we can write for the color component \mathbf{C}_i :

$$\mathbf{C}_i = \sum_{b=0}^{B-1} \sum_{l \in \mathbb{Z}} y_b^{C_i}[l] \mathbf{s}_b^{(i)}, \quad \mathbf{C}_i^{rec} = \sum_{b=0}^{B-1} \sum_{l \in \mathbb{Z}} \hat{y}_b^{C_i}[l] \mathbf{s}_b^{(i)}. \quad (23)$$

\mathbf{C}_i here is the color component in vector form after lexicographic ordering. $\mathbf{s}_b^{(i)}$ are the SBT synthesis vectors. Also the sum on l is on all the coefficient indices in the subband, $y_b^{C_i}[l]$ denotes the subband b

coefficient of \mathbf{C}_i at index l and $\hat{y}_b^{C_i}[l]$ is the same coefficient after quantization and reconstruction. Now consider the expression $E \left[\frac{1}{N} \langle \mathbf{C}_i - \mathbf{C}_i^{rec}, \mathbf{C}_j - \mathbf{C}_j^{rec} \rangle \right]$ for $i \neq j$, where N is the number of the image pixels. Using Equation (23), it can be written as:

$$E \left[\frac{1}{N} \langle \mathbf{C}_i - \mathbf{C}_i^{rec}, \mathbf{C}_j - \mathbf{C}_j^{rec} \rangle \right] = \frac{1}{N} \sum_{b=0}^{B-1} \sum_{p=0}^{B-1} \sum_{l \in \mathbb{Z}} \sum_{m \in \mathbb{Z}} E \left(\delta y_b^{C_i}[l] \delta y_p^{C_j}[m] \right) \langle \mathbf{s}_b^{(i)}, \mathbf{s}_p^{(j)} \rangle, \quad (24)$$

where $\delta y_b^{C_i}[l] \triangleq y_b^{C_i}[l] - \hat{y}_b^{C_i}[l]$. Assuming zero correlation of the quantization errors of the different color components in each subband and between subbands means that $E \left(\delta y_b^{C_i}[l] \delta y_p^{C_j}[m] \right) = 0$, hence $E \left[\frac{1}{N} \langle \mathbf{C}_i - \mathbf{C}_i^{rec}, \mathbf{C}_j - \mathbf{C}_j^{rec} \rangle \right] = 0$ immediately follows according to (24). But this means exactly zero correlation of the quantization errors in image domain. Thus the derivation of the WMSE expression of (21) is once again consistent with the derivation of the MSE expression of (4).

Basic Optimization Using the WMSE Model

After deriving the WMSE expression, the natural next step is to use it to find the optimal rates and optimal CCT in the WMSE sense. First we wish to minimize the WMSE of (21), subject to the rate constraint $\sum_{i=1}^3 \sum_{b=0}^{B-1} \eta_b R_{bi} = R$, resulting in the following Lagrangian (λ is the Lagrange multiplier):

$$L(\{R_{bi}\}, \bar{\mathbf{M}}, \lambda) = \frac{1}{3} \sum_{b=0}^{B-1} \sum_{k=1}^3 \eta_b G_b \sigma_{bk}^2 \varepsilon_k^2 e^{-aR_{bk}} \psi_{bk} + \lambda \left(\sum_{i=1}^3 \sum_{b=0}^{B-1} \eta_b R_{bi} - R \right), \quad (25)$$

which is minimized by the optimal rates given by:

$$R_{bi} = \frac{R}{3} + \frac{1}{a} \ln \left(\frac{G_b \sigma_{bi}^2 \varepsilon_i^2 \psi_{bi}}{\prod_{k=1}^3 (GM_k \varepsilon_k^2 \Psi_k)^{\frac{1}{3}}} \right) \quad (26)$$

Here

$$GM_k \triangleq \prod_{b=0}^{B-1} (G_b \sigma_{bk}^2)^{\eta_b} \quad \text{and} \quad \Psi_k \triangleq \prod_{b=0}^{B-1} (\psi_{bk})^{\eta_b}. \quad (27)$$

Note that no constraints for non-negativity of the rates are used here, which means that high rates R are assumed. As for the optimal CCT matrix $\bar{\mathbf{M}}$: it can be found by minimizing the target function $f(\bar{\mathbf{M}})$, that is actually the denominator of the $\ln()$ in (26) after some straightforward manipulations:

$$f(\bar{\mathbf{M}}) = \prod_{k=1}^3 (GM_k \Psi_k) = \prod_{k=1}^3 \prod_{b=0}^{B-1} (G_b \sigma_{bk}^2 \psi_{bk})^{\eta_b}. \quad (28)$$

We should remind here that ψ_{bk} is a function of $\bar{\mathbf{M}}$ as given in (20). Also the variances σ_{bk}^2 depend on $\bar{\mathbf{M}}$, or more specifically on \mathbf{M} . These variances are the diagonal elements of the subband b covariance matrix in the C1C2C3 image domain:

$$\tilde{\Lambda}_b \triangleq E[(\mathbf{Y}_b - \tilde{\mu}_{Y_b})(\mathbf{Y}_b - \tilde{\mu}_{Y_b})^T] \quad \tilde{\mu}_{Y_b} \triangleq E[\mathbf{Y}_b] \quad (29)$$

and can also be expressed using the \mathbf{M} matrix and the subband b covariance matrix in the RGB image domain:

$$\Lambda_b \triangleq E\left[(Y_b^{RGB} - \mu_{Y_b}^{RGB})(Y_b^{RGB} - \mu_{Y_b}^{RGB})^T\right], \quad (30)$$

$$(\mu_{Y_b}^{RGB} \triangleq E[Y_b^{RGB}])$$

according to:

$$\sigma_{bk}^2 = \mathbf{m}_k^T \Lambda_b \mathbf{m}_k. \quad (31)$$

Here $\mathbf{Y}_b^{RGB} = [Y_b^R Y_b^G Y_b^B]^T$ is defined similarly to the definitions in the beginning of the section of \mathbf{Y}_b . Also \mathbf{m}_k denotes the k^{th} row of the \mathbf{M} matrix in vector form. Thus the target function $f(\bar{\mathbf{M}})$ can be rewritten as:

$$f(\bar{\mathbf{M}}) = \prod_{k=1}^3 \prod_{b=0}^{B-1} \left((\mathbf{m}_k^T \Lambda_b \mathbf{m}_k) G_b \psi_{bk} \right)^{\eta_b}, \quad (32)$$

$$\psi_{bk} = \sum_{i=1}^3 w_{bi} \left(\bar{\mathbf{M}}^{-1} \right)_{ik}^2.$$

Optimal Rates with Down-Sampling

When considering potential down-sampling of some of the color components, the rate constraint becomes (5) and the Lagrangian that incorporates this constraint, as well as constraints for the non-negativity of the subband rates, is:

$$L(\{R_{bi}\}, \mathbf{M}, \lambda, \{\mu_{bi}\}) = \frac{1}{3} \sum_{b=0}^{B-1} \sum_{k=1}^3 \eta_b G_b \sigma_{bk}^2 e^{-a R_{bk}} \psi_{bk} \quad (33)$$

$$+ \lambda \left(\sum_{i=1}^3 \alpha_i \sum_{b=0}^{B-1} \eta_b R_{bi} - R \right) - \sum_{i=1}^3 \sum_{b=0}^{B-1} \mu_{bi} R_{bi},$$

where μ_{bi} are the Lagrange multipliers for the new constraints. The rates that minimize (33) are:

$$R_{bi} = \frac{R}{\sum_{j=1}^3 \alpha_j \xi_j} \quad (34)$$

$$+ \frac{1}{a} \ln \left(\frac{\frac{\varepsilon_i^2 G_b \sigma_{bi}^2 \psi_{bk}}{\alpha_i}}{\prod_{k=1}^3 \left(\frac{GM_k^{Act} \varepsilon_k^2 \Psi_k^{Act}}{\alpha_k} \right)^{\sum_{j=1}^3 \alpha_j \xi_j}} \right),$$

where $b \in Act_i$ with Act_i defined in (7) while GM_k^{Act} and ξ_i are as in (8). As for Ψ_k^{Act} , it is given by:

$$\Psi_k^{Act} \triangleq \prod_{b \in Act_k} (\psi_{bk})^{\eta_b}. \quad (35)$$

Perceptually Optimized Compression

In this section we present a general approach to color image compression using a subband transform with perceptual optimization of the CCT and of the subband rates allocation. This approach consists of the stages described in the beginning of Section "Objective Rate-Distortion theory of subband transform coders". The differences here is that in the pre-processing stage, the perceptually optimal CCT transform is applied to the color components and in the quantization stage the perceptually optimal rates allocation is used. We demonstrate this approach both for the DCT and the DWT in the following subsections. Note that a probability distribution model can be used for the SBT coefficients to improve the performance of the algorithms with respect to run-time and compression quality [4]. For example, the Laplacian probability model can be assumed for DCT coefficients [9].

DCT-Based Compression Algorithm

Since the DCT is a subband transform, the Rate-Distortion theory of Section "The Perceptual R-D Model" can be applied to it. To find the DCT visual weights we use the HVS CSF (Contrast Sensitivity Function) curves for the YCbCr color space that can be found, for example, in [20]. To convert the cpd (cycle per degree) units of these graphs to spatial frequency units for the DCT, the equations proposed in [22] can be used. We consider, for example, 512×512 256×256 images displayed as $64mm \times 64mm$ on a display with dot pitch of 0.25mm. The viewing distance is assumed to be four times the image height [12], i.e., in this example 50cm. Similarly we can consider 512×512 images displayed as $128mm \times 128mm$ on a big screen at a viewing distance of 100cm.

The stages of the proposed algorithm are as follows:

1. Find the optimal CCT \mathbf{M} by minimizing (32).
2. Apply the CCT \mathbf{M} to the RGB color components of the image to receive the new color components $C1, C2, C3$.
3. Apply the DCT block transform to each color component $C_i, i \in \{1,2,3\}$.

4. Calculate the optimal rates according to (34) substituting there the used CCT matrix and the variances of the DCT subbands. To find the active subbands, the algorithm presented in [5] can be used.
5. Quantize the DCT coefficients using a uniform scalar quantizer in each subband. The (optimal) quantization steps are found using an iterative algorithm [5].
6. Use post-quantization coding similar to the one used in JPEG. Adaptive Huffman coding is employed and the codes are sent with the image data. This stage is lossless and does not affect the image distortion.

It is of interest to compare the performance of this algorithm to the other DCT-based compression algorithms, such as the MSE optimized algorithm proposed in [5] and JPEG. A comparison for several images is given in Table 1. We consider here the above algorithm with WMSE R-D optimization of the rates










allocation and CCT, as well as another version that uses optimal rates, but in the YCbCr color space. The PSPNR measure used here is:

$$PSPNR \triangleq 10 \log_{10} \frac{255^2}{WMSE} \quad (36)$$

where $WMSE$ for each color component is calculated in the DWT domain in the YCbCr color space according to the visual weights suggested in [20]. Then the average PSPNR on the 3 color components is taken. Based on our experience and results, this is a good measure of subjective image quality.

Note that each image in the table was compressed at the same compression rate (given in the last column from the left) for each of the algorithms, but the rate is not the same for different images. The reason is that the the rate was chosen to achieve the same objective performance (PSNR) for the first algorithm (from the left) to allow meaningful comparison of average algorithm performances. See also Table 2 below.

TABLE 1 Perceptually-based results (PSPNR) for (from left to right): The DCT-based WMSE optimized algorithm in the YCbCr domain; The same algorithm with optimal CCT; The MSE optimized algorithm; JPEG. The compression rate for each image is shown in the right column.

	Image	WMSE Alg. in the YCbCr domain	WMSE Alg. in the optimal domain	MSE Alg.	JPEG	Rate [bpp]
	Lena	39.4	40.6	38.9	37.6	0.76
	Peppers	39.6	39.6	38.1	36.6	0.81
	Baboon	42.0	42.5	39.2	36.1	1.76
	Cat	41.3	43.1	41.3	39.9	1.30
	Landscape	42.5	42.5	40.5	38.0	1.85
	House	39.8	40.3	39.2	38.1	0.54
	Jelly Beans	38.5	38.6	38.3	37.5	0.47
	Fruits	41.0	42.3	40.4	38.9	0.71
	Sails	41.0	42.9	39.7	37.6	1.84














	Monarch	39.8	40.2	38.7	37.5	1.03
	Goldhill	42.9	43.4	41.9	40.6	2.17
	Mean	40.7	41.5	39.7	38.0	

TABLE 2 Same as Table 1, but for PSNR instead of PSNR. Note that optimization of PSPNR, as induced by the human observer, does not necessarily mean optimization of the arbitrarily used PSNR (see text).

		PSNR				
	Image	WMSE Alg. in the YCbCr domain	WMSE Alg. in the optimal domain	MSE Alg.	JPEG	Rate [bpp]
	Lena	30.0	30.5	30.7	29.7	0.76
	Peppers	30.0	30.1	30.5	29.3	0.81
	Baboon	30.0	29.0	30.5	26.5	1.76
	Cat	30.0	29.6	31.3	29.5	1.30
	Landscape	30.0	30.1	30.3	25.9	1.85
	House	30.0	30.2	30.3	29.5	0.54
	Jelly Beans	30.0	30.3	30.6	29.7	0.47
	Fruits	30.0	29.8	30.6	30.6	0.71
	Sails	30.0	29.7	30.6	28.9	1.84
	Monarch	30.0	29.6	30.6	29.4	1.03
	Goldhill	30.0	30.2	31.7	29.2	2.17
	Mean	30.0	29.9	30.7	28.9	

It can be concluded from the table that the WMSE optimized algorithm with the optimal CCT achieves the highest PSPNR, which is 1.8dB higher on average than the PSPNR of the MSE optimized algorithm and 3.5dB above JPEG. The use of the optimal CCT in WMSE sense increases the performance by almost 1dB (0.8dB) on average when perceptually optimal rates are employed. Another comparison of interest is of the standard or objective distortions of the algorithm, i.e.,

the PSNR as presented in Table 2. As expected, the MSE optimized algorithm is superior here, but what is perhaps less intuitive is the fact that the use of the optimal CCT slightly decreases the PSNR, indicating that PSNR and PSPNR are different measures. As can be seen in the examples of Figs. 1 - 2 below, the human observer judgement is closely related to the PSPNR, not the PSNR. Despite this both WMSE algorithms have MSE performance superior to JPEG with a gain

of 1.1dB in the PSNR without using the optimal CCT and slightly less (1dB) with the optimal CCT. We conclude this section by presenting a visual comparison of the algorithms as can be seen in Fig. 1 for the Lena image and in Fig. 2 for the Baboon image.

It can be seen that the WMSE algorithm provides the best results for both images visually, while the results of the MSE algorithm are slightly less pleasing to the eye. Yet both algorithms are superior to JPEG.

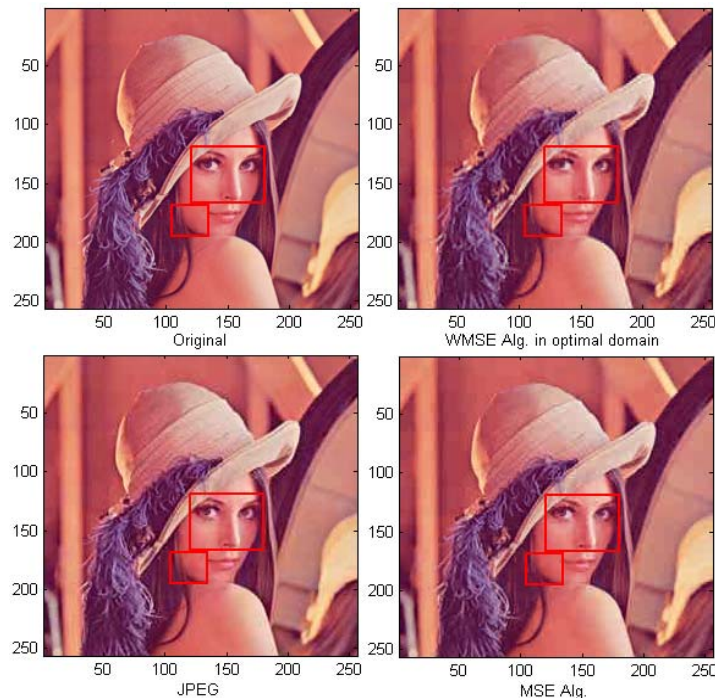


FIG. 1 COMPRESSION RESULTS FOR LENA AT 0.72 BPP. ORIGINAL IMAGE (TOP LEFT); IMAGE COMPRESSED BY THE WMSE OPTIMIZED ALGORITHM (TOP RIGHT, PSPNR=40.4DB); IMAGE COMPRESSED BY JPEG (BOTTOM LEFT, PSPNR=37.7DB); IMAGE COMPRESSED BY THE MSE OPTIMIZED ALGORITHM (BOTTOM RIGHT, PSPNR=39.3DB). AS EXPECTED, THE WMSE ALGORITHM OUTPERFORMS THE OTHER METHODS, ESPECIALLY IN THE MARKED AREAS.

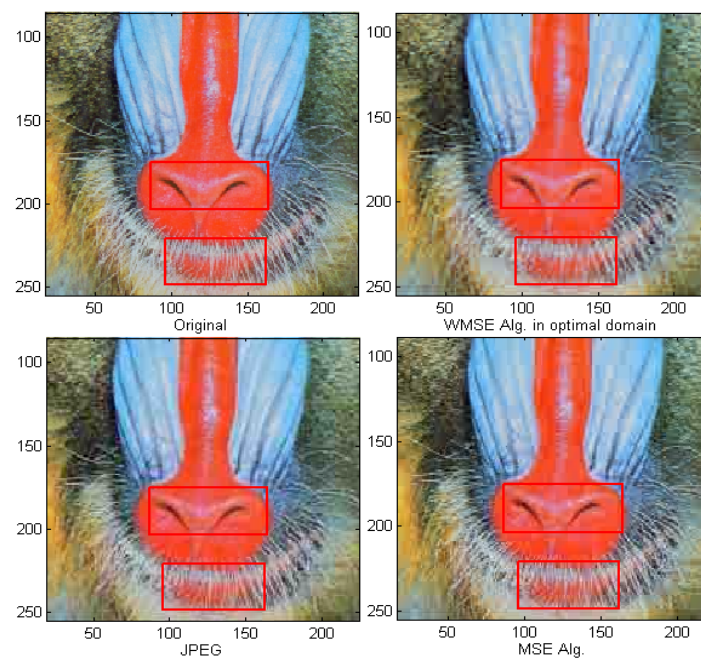


FIG.2 COMPRESSION RESULTS FOR THE BABOON (ZOOMED IN) AT 0.88 BPP. ORIGINAL IMAGE (TOP LEFT); IMAGE COMPRESSED BY THE WMSE OPTIMIZED ALGORITHM (TOP RIGHT, PSPNR=36.9DB); IMAGE COMPRESSED BY JPEG (BOTTOM LEFT, PSPNR=33.6DB); IMAGE COMPRESSED BY THE MSE OPTIMIZED ALGORITHM (BOTTOM RIGHT, PSPNR=35.6DB). HERE AGAIN, THE WMSE ALGORITHM OUTPERFORMS THE OTHER METHODS.

DWT-Based Compression Algorithm

When the DWT is considered, there are quite a few options for the wavelet filter bank to be used for the decomposition. We have chosen the Daubechies 9/7 filter bank, but obviously other choices can be considered as well. No tiling [13] is used. The choice of the visual weights is according to [20]. The stages of the proposed algorithm are:

1. Find the optimal CCT \mathbf{M} by minimizing (32).
2. Apply the CCT \mathbf{M} to the RGB color components of the image to receive the new color components $\mathbf{C1}$, $\mathbf{C2}$, $\mathbf{C3}$.
3. Apply the DWT tree decomposition up to the required depth of the tree (3, 4, 5 or higher according to image size) to each color component \mathbf{C}_i , $i \in \{1, 2, 3\}$.
4. Calculate the optimal rates according to (34) substituting there the used CCT matrix and the variances, sample rates and energy gains of the DWT subbands. The determination of the active subbands is the same as for the DCT-based algorithm of the previous subsection.

5. Quantize the DWT coefficients by a uniform quantizer with a central dead-zone in each subband similar to the one used in JPEG2000 Part I [8]. Use optimal quantization steps.

6. Use the post-quantization coding of the EZW algorithm [19] on the quantized subband coefficients. This stage is lossless and includes bit plane coding using zero trees. The bit plane coding is split into two passes (dominant and subordinate) and a separate arithmetic coder is employed for each pass.

It is interesting to compare the proposed algorithm to JPEG2000. We have considered the JPEG2000 implementation using the JasPer software package [24] and another version of the implementation with fixed visual weighting at subband level using the CSF weights of [20]. The visual results for the Lena image can be seen in Fig. 3. The PSNR results here are 29.5dB for the proposed WMSE optimized algorithm, 28.6dB for JPEG2000 (original JasPer implementation) and 28.5dB for JPEG2000 with CSF weights. We conclude that the use of CSF weights, that affects the tier-2 coding stage of the JPEG2000 algorithm, decreases the PSNR, but slightly improves the visual performance.

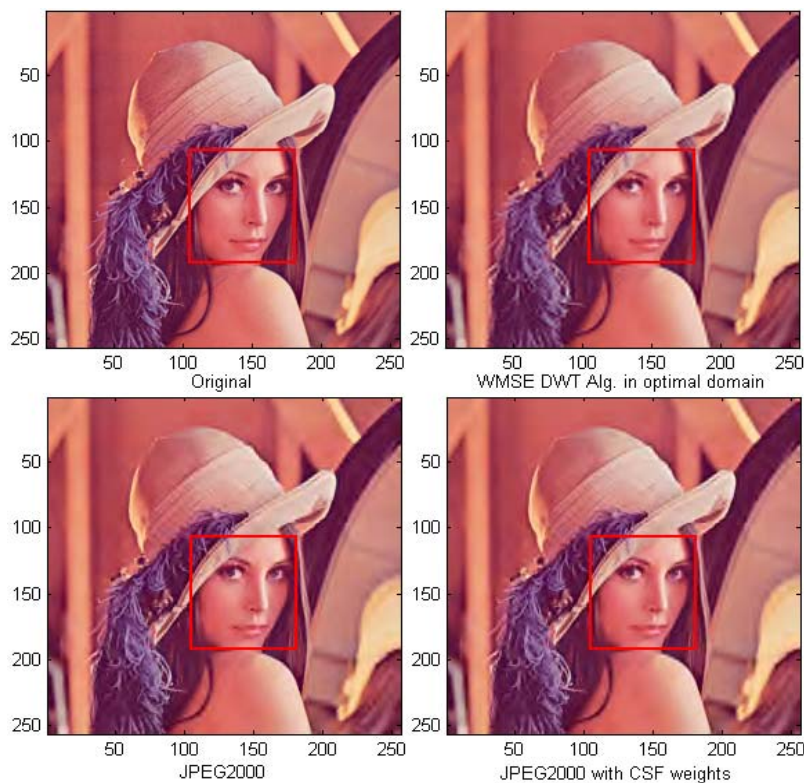


FIG.3 COMPRESSION RESULTS FOR LENA AT 0.52 BPP. ORIGINAL IMAGE (TOP LEFT); IMAGE COMPRESSED BY THE DWT-BASED WMSE OPTIMIZED ALGORITHM (TOP RIGHT, PSNR=19.7DB); IMAGE COMPRESSED BY JPEG2000 (BOTTOM LEFT, PSNR=19.1DB); IMAGE COMPRESSED BY JPEG2000 WITH CSF WEIGHTS (BOTTOM RIGHT, PSNR=19.2DB). ALSO HERE, THE WMSE ALGORITHM IS SUPERIOR TO THE REST.

Also the proposed algorithm produces an image that is much more pleasing to the eye than JPEG2000.

Similar results can be seen in the comparison of the proposed algorithm and JPEG2000 for other example images in Figs. 4, 5 and 6. In Fig. 4 the loss of spatial details at high frequencies in the Landscape and House images as well as the introduction of false contours in the Jelly Beans image should be noted for JPEG2000. These effects can be seen in the marked regions. In Fig. 5 once again the superiority of the WMSE optimized algorithm on JPEG2000 can be seen in regions of high frequency details as demonstrated by the Fruits and Cat images. For example, the details of the apple texture in the Fruits image and of the fur

and mustache textures in the Cat image are lost. In the case of the Peppers image, the compression result of JPEG2000 is less pleasing to the eye due to the color artifacts introduced. Fig. 6 further demonstrates the loss of spatial details in the case of JPEG2000 compression of the Sails image, the blurring of the contours in the Monarch image and both effects in the Goldhill image (see the top marked area for the blurred contour effect and, for example, the bottom left marked area for the loss of spatial details). Furthermore, color artifacts are introduced by JPEG2000 in the Goldhill image as indicated, for instance, in the marked area in the center of the image.

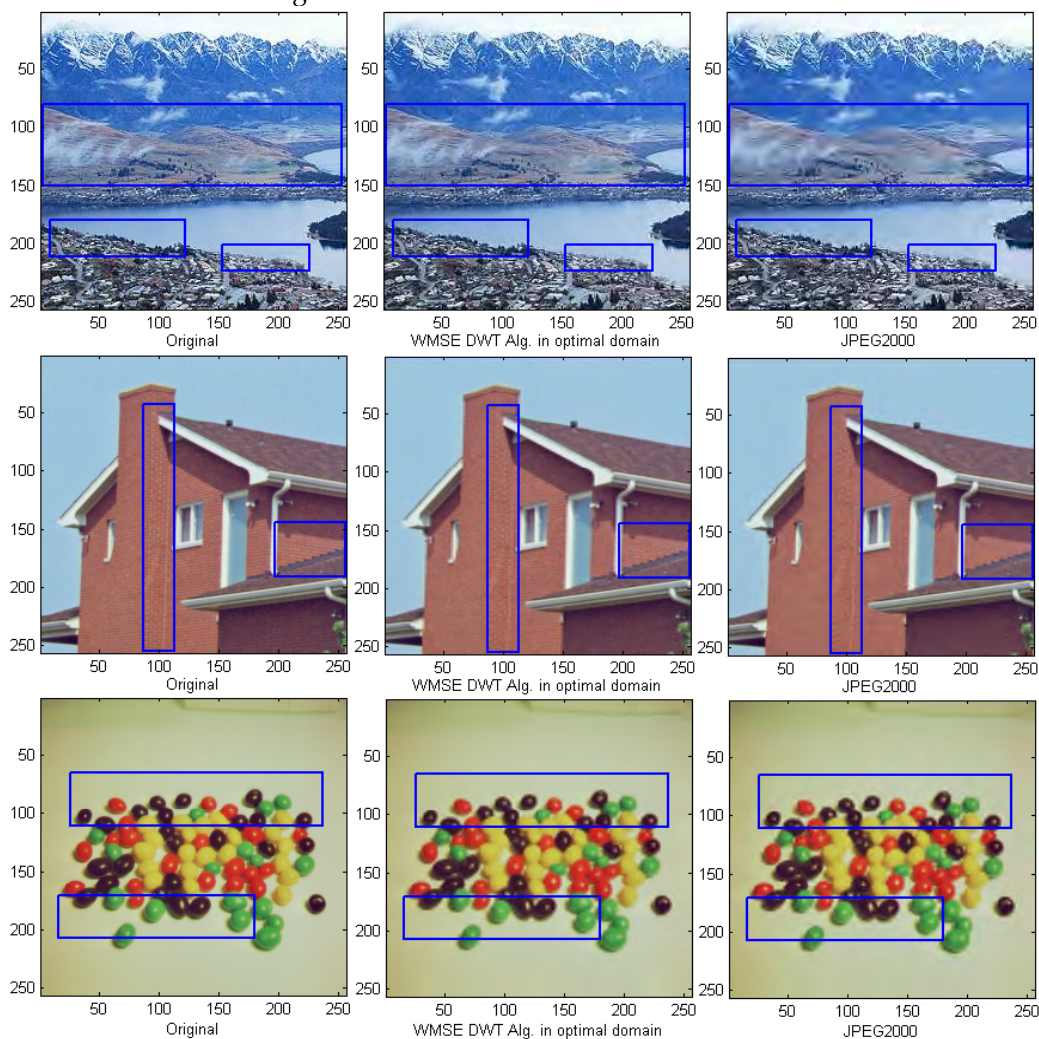


FIG.4 LANDSCAPE, HOUSE AND JELLY BEANS IMAGES - FROM LEFT TO RIGHT: ORIGINAL, COMPRESSED BY THE WMSE ALGORITHM (WMSE ALG.) AND COMPRESSED BY JPEG2000.

PSPNR FOR THE LANDSCAPE IMAGE: 17.1DB (WMSE ALG.) AND 15.7DB (JPEG2000).

PSNR: 28.7DB (WMSE ALG.) AND 25.3DB (JPEG2000) AT 0.97BPP.

PSPNR FOR THE HOUSE IMAGE: 19.4DB (WMSE ALG.) AND 19.0DB (JPEG2000).

PSNR: 31.2DB (WMSE ALG.) AND 33.1DB (JPEG2000) AT 0.68BPP.

PSPNR FOR THE JELLY BEANS IMAGE: 18.8DB (WMSE ALG.) AND 18.2DB (JPEG2000).

PSNR: 32.3DB (WMSE ALG.) AND 32.1DB (JPEG2000) AT 0.48BPP.

IN THE ONLY CASE WHERE THE PSNR OF JPEG2000 IS HIGHER THAN THE NEW ALGORITHM (HOUSE), THE PSNR RESULT SUPPORTS THE FACT THAT VISUALLY THE NEW ALGORITHM PROVIDES SUPERIOR RESULTS.

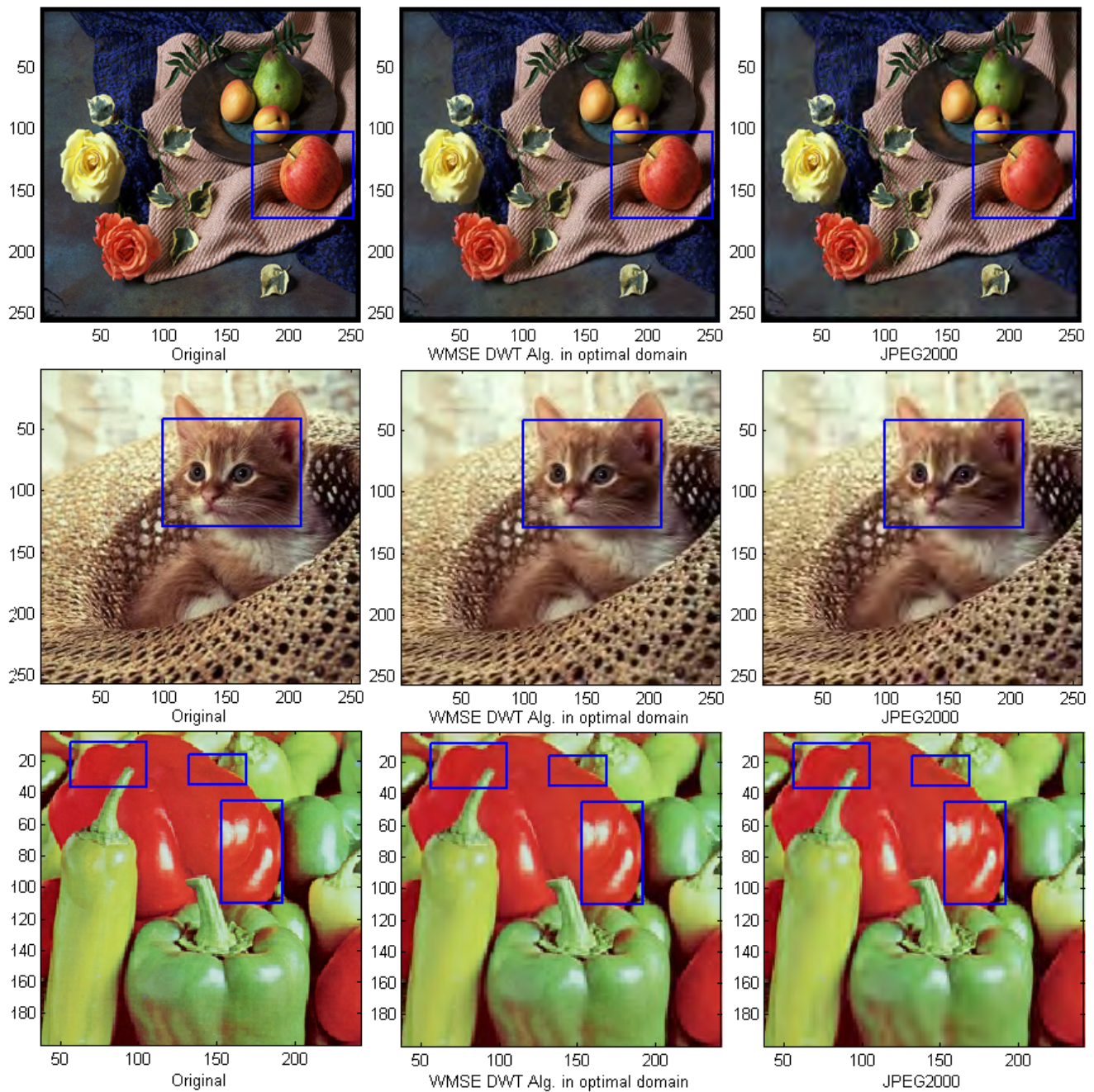


FIG. 5 FRUITS, CAT AND PEPPERS IMAGES - FROM LEFT TO RIGHT: ORIGINAL, COMPRESSED BY THE WMSE ALGORITHM (WMSE ALG.) AND COMPRESSED BY JPEG2000.

PSPNR FOR THE FRUITS IMAGE: 22.2DB (WMSE ALG.) AND 21.1DB (JPEG2000).

PSNR: 30.0DB (WMSE ALG.) AND 29.0DB (JPEG2000) AT 1.34BPP.

PSPNR FOR THE CAT IMAGE: 17.0DB (WMSE ALG.) AND 16.2DB (JPEG2000).

PSNR: 28.9DB (WMSE ALG.) AND 26.9DB (JPEG2000) AT 0.63BPP.

PSPNR FOR THE PEPPERS IMAGE: 20.3DB (WMSE ALG.) AND 19.3DB (JPEG2000).

PSNR: 30.8DB (WMSE ALG.) AND 30.7DB (JPEG2000) AT 0.86BPP.

AS CAN BE SEEN, PSNR AND PSPNR RESULTS ARE SUPERIOR FOR THE NEW ALGORITHM COMPARED TO JPEG2000. IT IS ALSO OBSERVED VISUALLY - EXAMPLES ARE INDICATED IN THE MARKED AREAS.



FIG. 6 SAILS (ZOOMED IN), MONARCH (ZOOMED IN) AND GOLDHILL IMAGES - FROM LEFT TO RIGHT: ORIGINAL, COMPRESSED BY THE WMSE ALGORITHM (WMSE ALG.) AND COMPRESSED BY JPEG2000.

PSPNR FOR THE SAILS IMAGE: 19.2DB (WMSE ALG.) AND 18.0DB (JPEG2000).

PSNR: 28.9DB (WMSE ALG.) AND 26.6DB (JPEG2000) AT 0.70BPP.

PSPNR FOR THE MONARCH IMAGE: 19.9DB (WMSE ALG.) AND 19.6DB (JPEG2000).

PSNR: 29.0DB (WMSE ALG.) AND 28.8DB (JPEG2000) AT 0.56BPP.

PSPNR FOR THE GOLDHILL IMAGE: 17.6DB (WMSE ALG.) AND 16.6DB (JPEG2000).

PSNR: 27.0DB (WMSE ALG.) AND 24.5DB (JPEG2000) AT 0.59BPP.

ONCE AGAIN, THE PSNR AND PSPNR RESULTS ARE SUPERIOR FOR THE NEW ALGORITHM COMPARED TO JPEG2000 (SEE EXAMPLES INDICATED IN THE MARKED AREAS).

Summary

A perceptually-based model for the Rate-Distortion function of color subband coders has been introduced. The new model approximates the WMSE distortion of an image in a given color space, such as YCbCr. This distortion is then minimized to achieve perceptual optimization of the compression. When the weights in the WMSE calculation are taken based on the CSF curves of the human visual system, better correspondence to image quality assessment by the human eye is achieved.

Based on the Rate-Distortion model, new algorithms have been introduced consisting of a pre-processing

stage using a CCT, followed by a subband transform, quantization stage, and lossless entropy encoding. The algorithms are optimized with regard to the color component transform in the pre-processing stage of the compression as well as the quantization tables used in the coding stage, both with respect to WMSE. The proposed DCT-based algorithm outperforms both JPEG and the corresponding MSE optimized algorithm. The DWT-based algorithm, as expected, achieves higher compression ratios for the same image quality than DCT-based techniques. We demonstrate in this work that even when a relatively basic algorithm is used in the post-processing stage (introduced for EZW), superior results are obtained by

the proposed algorithm when compared to other DWT-based algorithms, such as JPEG2000. This holds even if the same WMSE distortion is used in both JPEG2000 and the proposed algorithm. Our conclusion is that based on the new perceptual Rate-Distortion model, optimized compression algorithms can be designed with compression results superior to presently available techniques.

ACKNOWLEDGMENT

This research was supported in part by the HASSIP Research Program HPRN-CT-2002-00285 of the European Commission, and by the Ollendorff Minerva Center. Minerva is funded through the BMBF.

REFERENCES

- [1] Faugeras, O. D. "Digital Color Image Processing Within the Framework of a Human Visual Model." *IEEE Trans. on Acoustics Speech and Signal Processing ASSP-27* (1979): 380-393.
- [2] Fiorucci, F., Baruffa, G. and Frescura, F. "Objective and subjective quality assessment between JPEG XR with overlap and JPEG 2000.", *Journal of Visual Communication and Image Representation* 23 (Aug. 2012): 835-844.
- [3] Gershikov, E. and Porat, M. "A Rate-Distortion Approach to Optimal Color Image Compression." *Proc. of EUSIPCO, Florence, Italy, 2006*.
- [4] Gershikov, E. and Porat, M. "Data Compression of Color Images using a Probabilistic Linear Transform Approach", in *LNCS #4310*, T. Boyanov, S. Dimova, K. Georgiev, G. Nikolov (Eds.), 582-589, Springer-Verlag Berlin Heidelberg, 2007.
- [5] Gershikov, E. and Porat, M. "On color transforms and bit allocation for optimal subband image compression". *Signal Processing: Image Communication* 22 (2007): 1-18.
- [6] Gersho, A. and Gray, R. M. "Vector Quantization and Signal Compression", Boston, MA: Kluwer, 1992, ch. 2.
- [7] Goffman-Vinopal, L. and Porat, M. "Color image compression using inter-color correlation." *Proc. of IEEE ICIP* (2002): II-353 - II-356.
- [8] JPEG 2000 Part I: Final Draft International Standard (ISO/IEC JTC1/SC29/WG1 N1855 (Aug. 2000).
- [9] Lam, E. Y. and Goodman, J. W. "A mathematical analysis of the DCT coefficient distributions for images." *IEEE Trans. on Image Processing* 9 (2000): 1661-1666.
- [10] Limb J. O. and Rubinstein C.B. "Statistical Dependence Between Components of A Differentially Quantized Color Signal." *IEEE Trans. on Communications Com-20* (Oct. 1971): 890-899.
- [11] Mannos, J. and Sakrison, D. "The effects of a visual fidelity criterion of the encoding of images." *IEEE Trans. on Information Theory* 20 (Jul. 1974): 525-536.
- [12] Ngan, K. N., Leong, K. S. and Singh, H. "Adaptive cosine transform coding of images in perceptual domain." *IEEE Trans. on Acoustics, Speech, and Signal Processing* 37 (Nov. 1989): 1743-1750.
- [13] Rabbani, M. and Joshi, R. "An overview of the JPEG 2000 still image compression standard". *Signal Processing: Image Communication* 17 (2002): 3-48.
- [14] Rao, K. R. and Yip, P. "Discrete cosine transform: algorithms, advantages, applications." Academic Press, 1990.
- [15] Richter, T. and Simon, S. "On the JPEG 2000 ultrafast mode". *Proc. of ICIP* (Oct. 2012): 2501-2504.
- [16] Richter, T. "Spatial Constant Quantization in JPEG XR is Nearly Optimal". *Proc. Of the Data Compression Conference* (March 2010): 79-88.
- [17] Roterman, Y. and Porat, M. "Color image coding using regional correlation of primary colors". *Image and Vision Computing* 25 (2007): 637-651.
- [18] Satt, A. and Malah, D. "Design of Uniform DFT Filter Banks Optimized for Subband Coding of Speech", *IEEE Trans. on Acoustics, Speech and signal Processing* 37 (Nov. 1989): 1672-1679.
- [19] Shapiro, J. M. "Embedded Image Coding Using Zerotrees of Wavelet Coefficients", *IEEE Trans. on Signal Processing* 41 (1993): 3345-3462.

- [20] Taubman, D. S. and Marcellin, M. W. "JPEG2000: image compression, fundamentals, standards and practice", Kluwer Academic Publishers, 2002.
- [21] Wallace, G. K. "The JPEG still picture compression standard". IEEE Trans. Consumer Electronics 38 (1992): xviii-xxxiv.
- [22] Wang, C. Y., Lee, S. M. and Chang, L. W. "Designing JPEG quantization tables based on human visual system." Signal Processing: Image Communication 16 (2001): 501-506.
- [23] Yamaguchi, H. "Efficient Encoding of Colored Pictures in R, G, B Components." Trans. on Communications 32 (Nov. 1984): 1201-1209.
- [24] <http://www.ece.uvic.ca/mdadams/jasper>



Evgeny Gershikov received his Ph.D. in Electrical Engineering from Technion – Israel Institute of Technology in Haifa, Israel in 2011. His areas of interest are Signal and Image Processing, Color Processing and Vision, Computer Vision, Pattern Recognition and Speech

Recognition.